RSC Advances

ROYAL SOCIETY OF CHEMISTRY

www.rsc.org/advances

ARTICLE TYPE www. rsc.org/xxxxxx | XXXXXXXX

Structure-property relationships of aromatic polyamides and polythioamides: comparative consideration with those of analogous polyesters, polythioesters and polydithioesters†

Masayuki Nagasawa, Tatsuya Ishii, Daisuke Abe and Yuji Sasanuma*

Received Xth XXXXXXXXXX 20XX, Accepted Xth XXXXXXXXX 20XX
First published on the web Xth XXXXXXXXXX 200X
DOI: 10.1039/b000000x

Conformational characteristic and configurational properties of aromatic polyamides and polythioamides, analogues of common aromatic polyesters such as poly(ethylene terephthalate) and poly(trimethylene terephthalate), have been investigated *via* NMR experiments and molecular orbital calculations on model compounds and the refined rotational isomeric state calculations for the polymers. The polyamides and polythioamides were actually synthesized and characterized in terms of solubility, molecular weight, crystallinity, thermal transition, and thermal stability. Herein the experimental results are discussed mainly from the viewpoint of the conformational characteristics and compared with those obtained from analogous aromatic polyesters, polythioesters, and polydithioesters to reveal effects of heteroatoms O, S, and NH included in the backbone on the polymer structures and properties.

1 Introduction

In previous studies, we investigated conformational characteristics and configurational properties of aromatic polyesters [1–3] and designed, synthesized, and characterized novel aromatic polythioesters, and polydithioesters [4,5] (Fig. 1). The polyesters were early developed and have been produced on a large scale worldwide, whereas the polydithioesters have been quite recently brought forth. Each polymer has its own conformational characteristics, higher-order structures, physical properties, and functions; therefore, one may clearly distinguish a polymer from others, search for the synthetic scheme and molding process suitable for the polymer itself, and explore its applications. On the other hand, molecular designers may consider, for example, the aromatic polymers shown in Fig. 1 as analogues. This is because the polymers have similar skeletal structures and differ from each other only in the combination of two heteroatoms, X and Y.

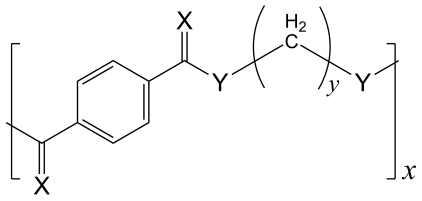

Fig. 1 Polymers treated here: polyamides (X = O and Y = NH), polyamide 2T (y = 2, abbreviated as PA2T) and polyamide 3T (y = 3, PA3T); polythioamides (X = S and Y = NH) polythioamide 2T (y = 2, PTA2T) and polythioamide 3T (y = 3, PTA3T); polyesters (X = Y = O), poly(ethylene terephthalate) (y = 2, PET) and poly(trimethylene terephthalate) (y = 3, PTT); polythioesters (X = O and Y = S) poly(ethylene dithioterephthalate) (y = 2, $P2TS_2$) and poly(trimethylene dithioterephthalate) (y = 3, $P3TS_2$); polydithioesters (X = S and Y = S) poly(ethylene tetrathioterephthalate) (y = 2, $P2TS_4$) and poly(trimethylene tetrathioterephthalate) (y = 3, $P3TS_4$).

This article deals mainly with four analogues, *i.e.,* aromatic polyamides and polythioamides of y = 2 and 3 (Figs. 1 and 2): polyamides 2T (PA2T) and 3T (PA3T); polythioamides 2T (PTA2T) and 3T (PTA3T). In the present study, we have employed the following investigative approaches: (1) molecular orbital (MO) calculations and NMR and single crystal X-ray diffraction experiments on small model compounds to reveal conformational characteristics of the polymers through the models; (2) the refined rotational isomeric state (RIS) calculations [6–8] for the polymeric chains to quantify their configu-

† Electronic Supplementary Information (ESI) available: Statistical weight matrices of PA2T and PTA2T (Appendix A) and PA3T and PTA3T (Appendix B); intramolecular interactions of 3DBA (Fig. S1) and 3DBTA (Fig. S2); solid-state ^{13}C NMR spectra observed from PA2T and PA3T (Fig. S3); molecular weight distributions of PTA2T and PTA3T (Fig. S4); geometrical parameters used in the refined RIS calculations for PA2T (Table S1), PTA2T (Table S2), PA3T (Table S3), PTA3T (Table S4), $P3TS_2$ (Table S5), and $P3TS_4$ (Table S6); averaged geometrical parameters of PA2T, PA3T, PTA2T, and PTA3T (Table S7) and $P2TS_2$, $P3TS_2$, $P2TS_4$, and $P3TS_4$ (Table S8).

Department of Applied Chemistry and Biotechnology, Graduate School and Faculty of Engineering, Chiba University, 1-33 Yayoi-cho, Inage-ku, Chiba 263-8522, Japan. E-mail: sasanuma@faculty.chiba-u.jp; Fax: +81-43-290-3394; Tel: +81-43-290-3394

rational properties and thermodynamic functions; (3) synthesis and characterization of the polymers to investigate their physical properties. Herein, the structures and properties of the aromatic polyesters, polythioesters, polydithioesters, polyamides, and polythioamides are compared and discussed as functions of X, Y, and *y*.

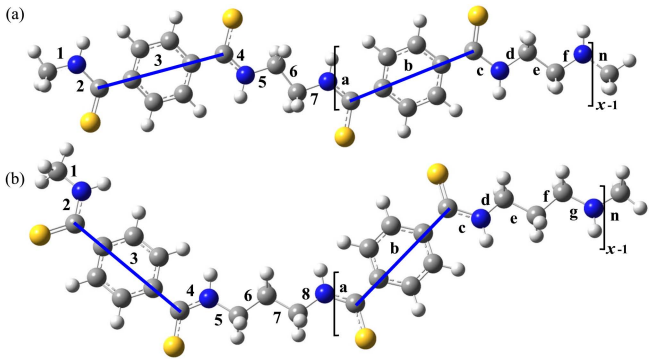

Fig. 2 All-trans states of (a) polyamide 2T (PA2T) or polythioamide 2T (PTA2T) and (b) polyamide 3T (PA3T) or polythioamide 3T (PTA3T). The thick line segment expresses the virtual bond of the aromatic ring. The bonds are labeled as indicated, and *x* is the degree of polymerization.

2 Methods

In general, the following experimental setup was employed here: a three- or four-necked flask (under a stream of dry nitrogen) equipped with a mechanical or magnetic stirrer, a dropping funnel, and a Dimroth condenser connected to a calcium chloride drying tube.

2.1 Synthesis of *N,N'*-ethylenedibenzamide (2DBA)[9]

Benzoyl chloride (5.6 g, 4.6 mL, 40 mmol), dissolved in dichloromethane (100 mL), was added dropwise to ethylenediamine (13 g, 14 mL, 220 mmol) and dichloromethane (300 mL) stirred in the flask dipped in ice water, and then the mixture was stirred at room temperature for 8 h. A white precipitate was collected by suction filtration, washed with distilled water, dried under reduced pressure at 40 °C, recrystallized from methanol, and dried *in vacuo* at 40 °C to yield 2DBA (2.9 g).

2.2 Synthesis of *N,N'*-trimethylenedibenzamide (3DBA)[10]

Benzoyl chloride (12.0 mL, 103 mmol) was added dropwise to 1,3-propane diamine (3.4 mL, 41 mmol) and aqueous sodium hydroxide (0.100 mol L^{-1}, 61.5 mL), and then the mixture was stirred at 0 °C for 1 h. After distilled water (100 mL) was added, the solution was stirred at room temperature overnight. A white precipitate was collected by suction filtration, rinsed with distilled water, dried under reduced pressure at 40 °C, recrystallized from a mixed solvent of ethanol and toluene (1 : 1 in volume), and dried *in vacuo* at 40 °C to yield 3DBA (3.1 g).

2.3 Synthesis of *N,N'*-ethylenedibenzothioamide (2DBTA)[11]

The 2DBA (1.0 g, 3.7 mmol) prepared as above and Lawesson's reagent (1.8 g, 4.5 mmol) were dissolved in toluene (20 mL) and stirred at 110 °C for 8 h. A yellow precipitate was collected by suction filtration, washed with toluene, dried under reduced pressure at 40 °C, recrystallized from ethanol, and dried *in vacuo* at 40 °C to yield 2DBTA (0.89 g).

2.4 Synthesis of *N,N'*-trimethylenedibenzothioamide (3DBTA)

In place of 2DBA, 3DBA was used and treated as described above; however, the crude product was purified differently. The reaction mixture was concentrated and underwent column chromatography using chloroform as the eluent, and yellowish fractions (retardation factor R_f = 0.3) were collected, concentrated, dried under reduced pressure at 40 °C, recrystallized twice from a mixed solvent of ethyl acetate and diethyl ether (1 : 1 in volume), and dried *in vacuo* to give 3DBTA (yield 48%).

2.5 Synthesis of Polyamides 2T (PA2T) and 3T (PA3T)

These two polyamides were synthesized by interfacial polycondensation of terephthaloyl chloride with ethylenediamine (PA2T) or 1,3-propanediamine (PA3T) according to Shashoua and Eareckson.[12]

2.6 Synthesis of Polythioamides 2T (PTA2T) and 3T (PTA3T)[13]

The synthetic procedure is common to PTA2T and PTA3T except for the starting material: PTA2T, ethylenediamine; PTA3T, 1,3-propanediamine. Sulfur powder (1.6 g, 50 mmol), *N,N'*-dimethylacetamide (70 mL, 0.76 mol), molecular sieve A4 (10 g), and ethylenediamine or 1,3-propanediamine (20 mmol) were mixed and stirred for 1 h, and then terephthalaldehyde (2.7 g, 20 mmol), dissolved in *N,N'*-dimethylacetamide (30 mL), was added dropwise. The solution was heated at 120 °C for 6 h. After being cooled down to room temperature, the reaction mixture was poured into methanol to yield a precipitate, which was collected by filtration, extracted with *N,N'*-dimethylformamide, and poured into methanol again. The precipitate was collected and rinsed with chloroform, carbon

disulfide, and distilled water. The purification was performed once again and dried *in vacuo* at 40 °C to yield PTA2T (22%) or PTA3T (41%).

According to the reaction mechanism proposed,[13] during the polymerization, water should preferably be eliminated as much as possible; therefore, we put molecular sieve A4 in the flask so that it would adsorb water and promote the reaction.

2.7 Synthesis of *N,N'*-dibenzylideneethylenediamine (DB2A) and *N,N'*-dibenzylidene-1,3-propanediamine (DB3A)[14]

Ethylenediamine or 1,3-propanediamine (9.7 mmol) was added to distilled water (30 mL) including benzaldehyde (2.2 mL, 21 mmol), and the mixture was stirred for 2 h to separate into aqueous and oily organic layers. The latter phase was recrystallized from *n*-hexane to generate white crystals, which were collected by suction filtration and dried *in vacuo* to yield DB2A (29%) or DB3A (35%).

2.8 Solution NMR

^{1}H (^{13}C) NMR spectra were recorded at 500 MHz (125.7 MHz) on a JEOL JNM-ECA500 spectrometer equipped with a variable temperature controller in the Center for Analytical Instrumentation of Chiba University. The sample temperatures were 25, 35, 45, and 55 °C and maintained within ±0.1 °C fluctuations. Free induction decays were accumulated 64 (256) times. The pulse duration, data acquisition time, and recycle delay were typically 5.7 (3.3) μs, 3.5 (0.8) s, and 5.0 (2.0) s, respectively. In the ^{13}C NMR experiments, the gated decoupling technique was used under the conditions written in the above parentheses. Because of poor solubilities of the model compounds, only dimethyl-d_6 sulfoxide (DMSO-d_6) was used as the NMR solvent. The NMR spectra were simulated with the gNMR program[15] to determine chemical shifts and coupling constants.

2.9 Solid state NMR

High-resolution ^{13}C cross polarization (CP) NMR experiments with magic angle spinning (MAS), abbreviated as CP/MAS, were carried out at a resonance frequency of 150.9 MHz on a JEOL JNM-ECA 600 spectrometer in the Center for Analytical Instrumentation of Chiba University. The sample was packed in a silicon nitride rotor of 4 mm in diameter and underwent a CP/MAS measurement under the following conditions: ^{1}H decoupler pulse duration, 3.5 μs; contact time, 3.0 ms; relaxation delay, 20 s; accumulation, 300 times; spinning rate, 17.0 kHz.

2.10 Solubility test

Solubilities of PA2T, PTA2T, PA3T, and PTA3T were examined for a number of solvents. Powdered polymer (2.0 mg) and a given solvent (1.0 mL) were mixed (solute concentration was 2.0 g L^{-1}) and stirred at room temperature. When the powder did not completely dissolve in the solvent at room temperature, the mixture was heated up to a temperature close to the boiling point of the solvent with being agitated. When the polymer still remained undissolved, the solubility was judged to be insoluble.

2.11 Size exclusion chromatography (SEC)

Inasmuch as PTA2T and PTA3T are soluble in some polar solvents, SEC measurements were conducted for these two polymers by Japan Analytical Industry Co., Ltd. (JAI) using a JAI LC9110 NEXT Recycling Preparative HPLC coupled with JAIGEL-3H-AF and 4H-AF columns. Each polythioamide (5.0 mg) was dissolved in *N,N*-dimethylformamide (DMF, 1.0 mL) containing LiBr (20 mM), purified with a 0.45 μm membrane filter, and injected into the HPLC. The LiBr additive prevents the polymer from aggregating, and the elute was fed at a rate of 1.0 mL min^{-1}. The columns were calibrated with polystyrene standards of molecular weights (M^{PS}'s) = 370, 2032, 13000, 100000, and 600000 according to a cubic polynomial: $\log M^{\mathrm{PS}} = A\tau^3 + B\tau^2 + C\tau + D$, where A, B, C, and D are empirical parameters and τ is the elution time. A JAI RI-700 NEXT and a JAL UV-370 (at 268 nm) detectors were used. The number-average (M_{n}) and weight-average (M_{w}) molecular weights were calculated by the built-in software JAI JDS-300.

2.12 Wide-angle X-ray diffraction

X-ray diffraction measurements were carried out by $\theta - 2\theta$ scans on a Bruker D8 Advance powder diffractometer. The incident X-ray beam was a Cu Kα line generated at 40 kV and 40 mA. The powdered specimen was put on a glass sample holder. The diffracted X-rays were detected by a scintillation counter.

2.13 Thermogravimetry (TG) and differential scanning calorimetry (DSC)

Thermogravimetric measurements were carried out with a Rigaku Thermo plus EVO II TG8120 under nitrogen atmosphere at a heating rate of 10 °C min^{-1}. Differential scanning calorimetric curves were recorded with a MAC DSC-3100 under nitrogen gas flow on first heating, first cooling, and second heating runs at a rate of 10 °C min^{-1}.

2.14 MO calculations

Density functional theory (DFT) and *ab initio* MO calculations were carried out with the Gaussian09 program[16] installed on an HPC Silent-SCC T2 or a HITACHI SR16000 computer in the Institute of Management and Information Technologies of Chiba University. For each conformer of the model compounds surrounded by dimethyl sulfoxide (DMSO) molecules, the geometry was fully optimized at the B3LYP/6-311+G(2d,p) level[17] with the self-consistent reaction field (SCRF) method using the conductor-like polarizable continuum model (CPCM),[18] and the thermal-correction term to the Gibbs free energy (at 25 °C) was also calculated. All self-consistent field (SCF) calculations were conducted under the tight convergence. With the optimized geometry, the electronic energy was computed at the MP2/6-311+G(2d,p)[19] and M062X/6-311+G(2d,p)[20] levels. The Gibbs free energy was evaluated from the electronic and thermal-correction energies, being expressed by ΔG_k (k: conformer) here as the difference from that of a given conformer. ^{1}H–^{1}H and ^{13}C–^{1}H coupling constants[21] of the model compounds for the NMR analysis were calculated at the B3LYP/6-311++G(3df,3pd) //B3LYP/6-311+G(3df,2p) level.

Herein, the dihedral angle is defined according to the tradition in polymer science:[6] trans (t) ~0°, gauche$^{\pm}$ (g$^{\pm}$) ~ ±120°, and cis (c) ~ 180°. The dihedral angle (ϕ) can be converted to that (Φ) recommended by International Union of Pure and Applied Chemistry[22] according to $\Phi = -\mathrm{sign}(\phi)(180 - |\phi|)$, where the function, sign(ϕ), returns the sign of ϕ, and *vice versa*: $\phi = -\mathrm{sign}(\Phi)(180 - |\Phi|)$. Non-SI units are used: free energy in kcal mol^{-1} (1 kcal mol^{-1} = 4.184 kJ mol^{-1}); bond length in Å (1 Å= 10^{-10} m).

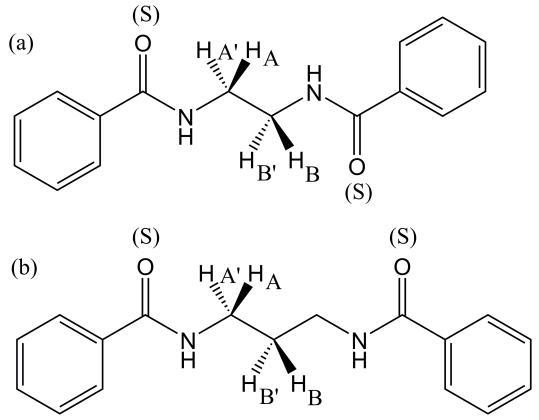

Fig. 3 Model compounds: (a) *N,N'*-ethylenedibenzamide (2DBA) and *N,N'*-ethylenedibenzothioamide (2DBTA) for PA2T and PTA2T, respectively; (b) *N,N'*-trimethylenedibenzamide (3DBA) and *N,N'*-trimethylenedibenzothioamide (3DBTA) for PA3T and PTA3T, respectively. The hydrogen atoms are partly designated to represent the NMR spin system.

3 Results and discussion

3.1 NMR of model compounds

Conformation- and configuration-dependent properties of a polymer in the Θ state (without the excluded volume effect) depend only on short-range intramolecular interactions,[6] which can be predicted both theoretically and experimentally from small model compounds with the same bond sequence as the polymer includes. In order to elucidate conformational characteristics of the polymers treated here, therefore, we carried out conformational analysis of their model compounds. The amide models are slightly soluble in methanol and well soluble in DMSO, trifluoroacetic acid (TFA) and 1,1,1,3,3,3-hexafluoro-2-propanol (HFIP), and hence DMSO-d_6 was used as the NMR solvent.

Fig. 4 shows ^{1}H NMR spectra observed from 2DBA, 2DBTA, 3DBA, and 3DBTA dissolved in DMSO at 25 °C. The gNMR simulations well reproduced the observed spectra and yielded chemical shifts and spin-spin coupling constants. Only vicinal coupling constants ($^3J^{\mathrm{NC}}$, $^3J_{\mathrm{HH}}$, and $^3J'_{\mathrm{HH}}$) needed for the conformational analysis are listed in Table 1. The N*H* signals of 2DBTA at 35 − 55 °C and 3DBTA at 55 °C were observed to collapse into a single peak, from which the $^3J^{\mathrm{NH}}$ value could not be derived; therefore, the corresponding lines of Tables 1 and 2 are blank.

From Newman projections in Fig. 5, the observed vicinal coupling constants can be related to trans (p_{t}) and gauche (p_{g}) fractions of the individual bonds:

$$^3J^{\mathrm{NC}} = \frac{J_{\mathrm{G}_1} + J_{\mathrm{G}_2}}{2} p_{\mathrm{t}} + \frac{J'_{\mathrm{E}} + J'_{\mathrm{G}}}{2} p_{\mathrm{g}} \quad (1)$$

$$^3J_{\mathrm{HH}} = {}^3J_{\mathrm{AB}} = {}^3J_{\mathrm{A'B'}} = J_{\mathrm{G}} p_{\mathrm{t}} + \frac{J'_{\mathrm{T}} + J''_{\mathrm{G}}}{2} p_{\mathrm{g}} \quad (2)$$

and

$$^3J'_{\mathrm{HH}} = {}^3J_{\mathrm{A'B}} = {}^3J_{\mathrm{AB'}} = J_{\mathrm{T}} p_{\mathrm{t}} + \frac{J'_{\mathrm{G}} + J'''_{\mathrm{G}}}{2} p_{\mathrm{g}} \quad (3)$$

where J_{T}'s, J_{G}', and J'_{E} are defined in Fig. 5. By definition, the following relation must be satisfied:

$$p_{\mathrm{t}} + p_{\mathrm{g}} = 1 \quad (4)$$

The coefficients, J_{T}'s, J_{G}', and J'_{E} were derived from two Karplus equations optimized for peptides,[23,24] DFT computations on the models, or experimental values of cyclic compounds, 2-methylpiperazine (2MPZ)[25] and 2-methylpiperidine (2MPD)[26] with −NH−CH_2−CH_2−NH− and −NH−CH_2−CH_2−CH_2−NH− bond sequences, respectively.

From eqs. 1 and 4, the p_{t} and p_{G} values of the N−CH_2 bond were determined, while those of the CH_2−CH_2 bond, derived from eqs. 2 and 3, were divided by the sum of p_{t} and p_{G} to satisfy eq. 4. The trans fractions (p_{t}'s) of both N−CH_2 and CH_2−CH_2 bonds, listed in Table 2, are seen to be sensitive to the J_{T}'s, J_{G}', and J'_{E} values employed in the analysis.

Table 1 Observed vicinal ^{1}H−^{1}H coupling constants of model compounds [a]

compound	temp, °C	$^3J^{NC}$	$^3J_{HH}$	$^3J'_{HH}$
2DBA	25	5.69	6.61	6.01
	35	5.70	6.62	6.02
	45	5.71	6.62	6.06
	55	5.72	6.62	6.14
2DBTA	25	5.40	6.10	5.79
	35[b]	–	6.03	5.81
	45[b]	–	5.96	5.57
	55[b]	–	5.68	5.34
3DBA	25	5.80	5.59	8.30
	35	5.80	5.60	8.30
	45	5.79	5.60	8.30
	55	5.79	5.60	8.30
3DBTA	25	5.50	5.42	8.64
	35	5.48	5.42	8.64
	45	5.47	5.42	8.64
	55[b]	–	5.42	8.64

[a] In Hz. [b] The signal from the NH proton collapsed into a broad singlet, from which no $^3J^{NC}$ value can be derived.

3.2 MO calculations on models

In the RIS approximation, the possible conformations of 2DBA and 2DBTA may be enumerated to be 3^3 (= 27); however, the molecular symmetry leaves us with only 10 irreducible conformations, for which the MO calculations were carried out at different levels and yielded the Gibbs free energies as shown in Table 3. The numbers of allowed conformers of 2DBA and 2DBTA are 6 and 8, respectively. The conformer free energy can be seen to depend largely on the MO theory. The trans fractions were also calculated from the ΔG_k values and compared with the NMR data (Table 2). Although the experimental p_t values, depending on the J_T's, J_G', and J'_E values, are somewhat scattered, the p_t's calculated from the B3LYP energies are found to fall within the range of or to be close to the experimental observations, whereas those of the CH_2−CH_2 bond from the MP2 and M062X methods are far from the experiment values.

The number of irreducible conformers of 3DBA and 3DBTA is 25, and the Gibbs free energies are listed in Table 4. The MP2 and M062X methods, compared with B3LYP, yield small ΔG_k values especially for $tg^+g^-g^-$, $g^+g^+g^+g^-$, $g^+g^+g^-g^+$, and $g^+g^+g^-g^-$. These four conformers of 3DBA and 3DBTA are, respectively, depicted in Figs. S1 and S2 (ESI), in which the following intramolecular interactions can be found: π/π (in $g^+g^+g^-g^-$ and $g^+g^+g^-g^+$); C-H$\cdots\pi$ ($tg^+g^-g^-$); NH$\cdots$O=C ($g^+g^+g^+g^-$). The MP2 and M062X methods probably overestimate these attractions; the corresponding ΔG_k energies were estimated to be so large negatives as to yield the extremely small p_t values of both N−CH_2 and CH_2−CH_2 bonds. It has often been pointed out that the MP2 theory tends to overestimate stabilities of π/π and CH$\cdots\pi$ attractions.[3,27–30] In contrast, the B3LYP energies provided the p_t values consistent with the NMR experiments.

The two −Y−C(=O) groups of aromatic polyesters (Y = O) and polythioesters (Y = S) are located on the benzene plane, and hence only two orientations, trans (dihedral angle ~ 0°) and cis (~ 180°), are allowed between the −Y−C(=O) groups connected to the same benzene ring.[1,4] In contrast, the geometrical optimizations for model compounds of the aromatic polydithioester (X = Y = S),[4,5] polyamides (X = O and Y = NH), and polythioamides (X = S and Y = NH) rendered the −Y−C(=X) groups out of the benzene plane. Therefore, the stereochemistry for the −Y−C(=X) groups must also be defined by another factor: the two C=X bonds are oriented in either the same (cis) direction or opposite (trans) directions with respect to the benzene plane. Four combinations of the former and latter factors are possible: trans-trans; trans-cis; cis-trans; cis-cis. However, the trans-cis and cis-trans combinations have two states with positive (+) and negative (−) dihedral angles: $(\text{trans-cis})^{\pm}$ and $(\text{cis-trans})^{\pm}$. Consequently, there are six states in all: trans-trans, $(\text{trans-cis})^{\pm}$, $(\text{cis-trans})^{\pm}$, and cis-cis (see Fig. 6).

The ΔG_k energies of the six states were evaluated from the MO calculations at the B3LYP/6-311+G(2d,p) level for more simplified models, *N,N'*-dimethylterephthalamide and *N,N'*-dimethylterephthalthioamide, and the dihedral angles

Table 2 Trans fractions (p_t's) of model compounds in DMSO

compound	temp, °C	p_t					
		N−CH_2			CH_2−CH_2		
		set A[a]	set B[b]	set C[c]	set a[d]	set b[e]	
		NMR expt					
2DBA	25	0.41	0.30	0.18	0.26	0.41	
	35	0.40	0.29	0.18	0.26	0.41	
	45	0.40	0.29	0.18	0.26	0.41	
	55	0.39	0.28	0.18	0.27	0.42	
2DBTA	25	0.56	0.44	0.30	0.28	0.45	
	35[f]	–	–	–	0.28	0.46	
	45[f]	–	–	–	0.27	0.45	
	55[f]	–	–	–	0.27	0.45	
3DBA	25	0.45	0.31	0.14	0.49	0.63	
	35	0.45	0.31	0.14	0.49	0.63	
	45	0.46	0.31	0.14	0.49	0.63	
	55	0.46	0.31	0.14	0.49	0.63	
3DBTA	25	0.52	0.40	0.32	0.53	0.69	
	35	0.53	0.40	0.32	0.53	0.69	
	45	0.53	0.41	0.33	0.53	0.69	
	55[f]	–	–	–	0.53	0.69	
		B3LYP[g]	MP2[h]	M062X[i]	B3LYP[g]	MP2[h]	M062X[i]
		MO calc					
2DBA	25	0.29	0.15	0.44	0.19	0.01	0.03
	35	0.29	0.15	0.44	0.19	0.01	0.04
	45	0.28	0.15	0.43	0.20	0.01	0.04
	55	0.28	0.16	0.43	0.20	0.01	0.04
2DBTA	25	0.32	0.42	0.40	0.31	0.02	0.08
	35	0.32	0.42	0.39	0.31	0.02	0.09
	45	0.32	0.41	0.39	0.31	0.02	0.09
	55	0.32	0.41	0.39	0.31	0.03	0.10
3DBA	25	0.22	0.03	0.04	0.61	0.02	0.08
	35	0.22	0.02	0.04	0.60	0.02	0.09
	45	0.22	0.03	0.05	0.60	0.03	0.10
	55	0.22	0.04	0.05	0.59	0.03	0.11
3DBTA	25	0.55	0.03	0.22	0.62	0.02	0.24
	35	0.54	0.03	0.23	0.62	0.02	0.25
	45	0.54	0.04	0.24	0.61	0.03	0.25
	55	0.53	0.04	0.24	0.60	0.03	0.26

[a-c]With the J_{G1}, J_{G2}, J_E, and J'_G values derived from Karplus equations of [a] Pardi *et al.*[23] and [b]Ludvigsen *et al.*[24] or [c] MO calculations for the model compounds. [d]With the J_T and J_G values obtained from NMR experiments on 2-methylpiperazine (for 2DBA and 2DBTA),[25] 2-methylpiperidine (for 3DBA and 3DBTA)[26] or [e] MO calculations for the model compounds. [f] The $^3J^{NC}$ value was not obtained. [g] The B3LYP/6-311+G(2d,p), [h] MP2/6-311+G(2d,p), or [i] M062X/6-311+G(2d,p) level using the geometry optimized at the B3LYP/6-311+G(2d,p) level with the solvent effect of DMSO.

were obtained from the MO calculations at the same level for 2DBA, 2DBTA, 3DBA, and 3DBTA. In Table 5, the data are compared with those on the aromatic polyesters, polythioesters, and polydithioesters. Regardless of polymer type, the ΔG_k differences between the six orientations are small, and hence the −Y−C(=X) group may be almost freely oriented in different directions, *i.e.,* freely rotatable around the benzene ring.

3.3 Configurational properties and thermodynamic quantities derived from the RIS calculations

The refined RIS scheme[8] that treats both geometrical parameters and energies as functions of conformations of the current and neighboring bonds has been applied to the aromatic polyamides, polythioamides, polythioesters, and polydithioesters to evaluate the characteristic ratio, configurational entropy, bond conformations, and average geometrical param-

Table 3 Free energies (ΔG_k's) of conformers of 2DBA and 2DBTA in DMSO, evaluated by MO calculations

					ΔG_k, kcal mol^{-1}					
					2DBA[a]			2DBTA[b]		
k	conformation[c]			M_k[d]	B3LYP[e]	MP2[f]	M062X[g]	B3LYP[e]	MP2[f]	M062X[g]
1	t	t	t	1				0.00	0.00	0.00
2	t	t	g^+	4				−0.12	−0.70	−0.27
3	t	g^+	t	2				−0.53	−1.71	−0.90
4	t	g^+	g^+	4						
5	t	g^+	g^-	4	0.00	0.00	0.00	−0.70	−3.88	−2.38
6	g^+	t	g^+	2	0.49	2.21	1.79	0.11	−0.96	−0.48
7	g^+	t	g^-	2	0.89	2.63	2.14	−0.73	−1.73	−1.14
8	g^+	g^+	g^+	2	0.59	1.67	1.35	−0.76	−2.53	−1.58
9	g^+	g^+	g^-	4	1.03	1.67	1.93	−0.39	−2.72	−1.17
10	g^+	g^-	g^+	2	1.64	−0.91	2.44			

[a]Relative to the tg^+g^- conformation. [b]Relative to the all-trans conformation. [c]In the HN−C−C−NH bond sequence. Both C=X (X = O or S) bonds were oriented to be trans-trans. The blank represents that the potential minimum was not found by the geometrical optimization at the B3LYP/6-311+G(2d,p) level. [d]Multiplicity. [e]At the B3LYP/6-311+G(2d,p) level. [f]At the MP2/6-311+G(2d,p) level. [g]At the M062X/6-311+G(2d,p) level.

Table 4 Free energies (ΔG_k's) of 3DBA and 3DBTA in DMSO, evaluated by MO calculations

						ΔG_k [a]					
						3DBA			3DBTA		
k	conformation[b]				M_k[c]	B3LYP[d]	MP2[e]	M062X[f]	B3LYP[d]	MP2[e]	M062X[f]
1	t	t	t	t	1	0.00	0.00	0.00	0.00	0.00	0.00
2	t	t	t	g^+	4	−0.54	−0.83	−0.62	1.19	0.75	1.06
3	t	t	g^+	t	4				1.07	0.65	0.87
4	t	t	g^+	g^+	4	0.32	−0.68	−0.32	1.92	0.81	1.30
5	t	t	g^+	g^-	4	0.57	−0.57	−0.17	1.37	0.31	1.03
6	t	g^+	t	g^+	4				1.28	−0.86	−0.29
7	t	g^+	t	g^-	4				1.89	0.97	1.53
8	t	g^+	g^+	t	2				1.03	−0.45	0.59
9	t	g^+	g^+	g^+	4				2.37	0.41	1.30
10	t	g^+	g^+	g^-	4	0.68	−1.62	−0.29			
11	t	g^+	g^-	t	2				4.70	0.56	2.85
12	t	g^+	g^-	g^+	4						
13	t	g^+	g^-	g^-	4	1.11	−2.09	−0.27	2.89	−0.98	1.40
14	g^+	t	t	g^+	2	−0.32	−0.91	−0.60	1.45	0.52	1.22
15	g^+	t	t	g^-	2	−0.34	−0.88	−0.36	0.97	−0.02	0.75
16	g^+	t	g^+	g^+	4	0.85	−0.45	0.30	1.83	−0.31	0.80
17	g^+	t	g^+	g^-	4	−0.11	−1.46	−0.71	1.84	0.07	1.21
18	g^+	t	g^-	g^+	4	0.34	−0.92	−0.32			
19	g^+	t	g^-	g^-	4	0.63	−0.56	−0.11	1.84	0.46	1.29
20	g^+	g^+	g^+	g^+	2	0.76	−1.10	−0.39	2.33	0.21	1.23
21	g^+	g^+	g^+	g^-	4	−0.29	−4.03	−2.74	1.57	−2.63	−0.82
22	g^+	g^+	g^-	g^+	4	1.69	−2.81	−0.39	3.32	−3.04	0.44
23	g^+	g^+	g^-	g^-	2	2.69	−0.55	1.44	3.77	−0.40	2.45
24	g^+	g^-	g^+	g^-	2						
25	g^+	g^-	g^-	g^+	2						

[a]Relative to the all-trans conformation. [b]In the HN−C−C−C−NH bond sequence. Both C=X (X = O or S) bonds were oriented to be trans-trans. The blank represents that the potential minimum was not found by the geometrical optimization at the the B3LYP/6-311+G(2d,p) level. [c]Multiplicity. [d]At the B3LYP/6-311+G(2d,p) level. [e]At the MP2/6-311+G(2d,p) level. [f]At the M062X/6-311+G(2d,p) level.

Table 5 Dihedral angles (ϕ), free energies (ΔG's), and conformational fractions (p_{conf}'s) around the benzene ring (bonds 3 and b) of the aromatic polyamides, polythioamides, polythioesters, and polydithioesters at 25 °C

			C=X (X = O or S) orientation: ξ			
			trans-trans	trans-cis$^{\pm}$	cis-trans$^{\pm}$	cis-cis
polyamide	ϕ_ξ [a]	PA2T	0.00	±53.6	±123.0	180.0
		PA3T	0.00	±46.9	±129.2	180.0
	ΔG_ξ [b]		0.00	−0.10	−0.38	0.08
	p_ξ [c]		0.12	0.15	0.24	0.11
polythioamide	ϕ_ξ [a]	PTA2T	0.00	±79.6	±98.0	180.0
		PTA3T	0.00	±75.8	±102.5	180.0
	ΔG_ξ [b]		0.00	−0.19	−0.32	−0.14
	p_ξ [c]		0.12	0.16	0.20	0.15
polyester[d]	ϕ_ξ [a]	PET	0.00			180.0
		PTT	0.00			180.0
	ΔG_ξ [b]		0.00			0.15
	p_ξ		0.56			0.44
polythioester[d]	ϕ_ξ [a]	P2TS$_2$	0.00			180.0
		P3TS$_2$	0.00			180.0
	ΔG_ξ [b]		0.00			0.15
	p_ξ		0.56			0.44
polydithioester	ϕ_ξ [a]	P2TS$_4$	0.00	±71.5	±106.3	180.0
		P3TS$_4$	0.00	±70.8	±106.3	180.0
	ΔG_ξ [b]		0.00	−0.10	0.15	0.05
	p_ξ [c]		0.17	0.20	0.13	0.16

[a]In deg. [b]In kcal mol^{-1}. Relative to the trans-trans orientation. [c]Because of the rounding error, the sum of p_ξ's does not exactly agree with unity. [d]The −S-C=O groups are located on the benzene plane; thus, only two states, trans and cis orientations, are defined for the polyesters and polythioesters.

eters. The statistical weight matrices of the polymers are formulated in Appendices A and B (ESI), and the geometrical parameters are tabulated in Tables S1 − S6 (ESI). Because the ΔG_k energies at the B3LYP/6-311+G(2d,p) level (Tables 3 and 4) well reproduced the NMR experiments, the B3LYP free energies were employed in the RIS calculations for the polyamides and polythioamides, together with those of the six orientations (Table 5). For the energy parameters of the polythioesters and polydithioesters, see the original papers.[4,5] The data on the polyesters are quoted from the literature.[1,3]

The characteristic ratios ($< r^2 >_0 / nl^2$'s) and configurational entropies (S_{conf}'s) are shown in Table 6, and the $< r^2 >_0 / nl^2$ ratios were calculated with the virtual bond connecting the two C=X (X = O or S) carbons (see Fig. 2); thus, the $< r^2 >_0 / nl^2$ values here can not be simply compared with those of nonaromatic polymers. Inasmuch as the statistical weight matrices were formulated with the ΔG_k energies, the p_t and p_ξ values given in Tables 2 and 5 are applicable as they are to the corresponding polymers. The geometrical parameters averaged over the exiting conformations are listed in Tables S7 and S8 (ESI). These theoretical data will be discussed later to interpret the following characterization of the polymers.

3.4 Synthesis and identification of PA2T and PA3T

The two polyamides were synthesized by interfacial polycondensation between terephthaloyl chloride and diamines according to Shashoua and Eareckson,[12] who estimated molecular weights of the polyamides by turbidimetry as 17.8 kDa (PA2T) and 23.7 kDa (PA3T). In Fig. S3 (ESI), solid-state ^{13}C NMR spectra of the two polyamides are compared with solution spectra of the model compounds, and the observed signals, assigned as indicated there, clearly show the formation of the two polyamides. As will be stated below, PA2T and PA3T are soluble in only irritant solvents; thus, we avoided SEC measurements for these polyamides. However, both polymers are expected to have molecular weights comparable to those reported by Shashoua and Eareckson.

3.5 Synthesis and identification of PTA2T and PTA3T

The two polythioamides were synthesized by the Willgerodt-Kinder type reaction according to Kanbara *et al.*[13] In Fig. 7, solution ^{13}C NMR spectra of PTA2T and PTA3T are compared with those of the model compounds, and the observed peaks are assigned as indicated. It is suggested that the Willgerodt-Kinder type reaction often yields Schiff base polymers with the CH$_2$=N bond.[13] Therefore, we also prepared

Table 6 Characteristic ratios ($< r^2 >_0 / nl^2$'s) and configurational entropies (S_{conf}'s) of the unperturbed polymers at 25 °C

	$< r^2 >_0 / nl^2$	S_{conf} (cal K^{-1} mol^{-1})
$y = 2$ [a]		
PA2T	3.15	8.37
PTA2T	3.55	9.38
$P2TS_2$	16.7	4.87
$P2TS_4$	5.20	8.87
PET	2.63	7.12
$y = 3$ [a]		
PA3T	3.65	10.5
PTA3T	5.66	10.6
$P3TS_2$	10.5	8.40
$P3TS_4$	6.06	11.5
PTT	4.14	8.93

[a] The number of methylene units.

DB2A and DB3A as models for the Schiff base polymers and measured their NMR (see Fig. 7). No signals related to the CH_2 =N bond are found in the spectra of PTA2T and PTA3T; thus, the by-products were not generated.

3.6 Solubility of PA2T, PA3T, PTA2T, and PTA3T

Solubilities of the four polymers were investigated for common and some special solvents. Both polyamides and polythioamides are insoluble in water, alcohols, chloroform, and dichloromethane, and tetrahydrofuran but soluble in some acidic solvents used often for aromatic polyesters, *e.g.*, TFA, HFIP, and sulfuric acid as shown in Table 7. The polythioamides are superior in solubility to the polyamides and soluble in pyridine, *N,N*-dimethylformamide (DMF), *N,N*-dimethylacetamide (DMAc), DMSO, and *N*-methylpyrrolidone (NMP) as well as the above acidic solvents.

The polyamides are soluble only in so-called helix-breaking solvents for polypeptides, such as TFA and HFIP, and their model compounds are soluble in not only the helix breakers but also DMSO. In our studies,[1,4,5,31] the MP2 calculations have successfully yielded precise conformational energies of polyethers, polythioethers, polyamines, polyesters, polythioesters, and polydithioesters, except for aromatic polyesters with intramolecular π/π and CH$\cdots\pi$ attractions.[2,3] In this study, however, the MP2 theory seems to overestimate intramolecular N−H$\cdots$O=C and N−H$\cdots$S=C hydrogen bonds as well as π/π and C−H$\cdots\pi$ attractions (see Figs. S1 and S2). In contrast, the B3LYP functional tends to underestimate attractive interactions such as dispersion forces,[32] thus representing interactions of the amides and thioamides better than MP2 and giving the results consistent with the NMR experiments.

3.7 Molecular weights of PTA2T and PTA3T

The novel polymers, PTA2T and PTA3T, are soluble in some polar organic solvents and hence underwent SEC measurements. The molecular weight distributions of PTA2T and PTA3T are shown in Fig. S4 (ESI). The M_n and M_w values are, respectively, as follows: PTA2T, 10.7 kDa and 17.3 kDa; PTA3T, 13.9 kDa and 29.3 kDa. Accordingly, the polydispersity indexes can be estimated as 1.62 (PTA2T) and 2.11 (PTA3T).

As shown in Fig 8, films of PTA2T and PTA3T were cast on small petri dishes from the DMF solutions; therefore, the polythioamides have molecular weights enough to form the films, which are optically translucent and brown colored.

3.8 Crystals structures of model compounds

Crystal structures of 2DBA and 3DBA were determined by Brisse *et al.*,[33,34] and those of 2DBTA and 3DBTA by us[35,36] (see Fig. 9). In the crystal, 2DBA, 2DBTA, 3DBA, and 3DBTA adopt, respectively, g^+tg^-, $g^+g^+g^+$, ttg^+g^+, and $tttg^+$ conformations, which were not necessarily suggested by the DFT calculations to be the lowest in ΔG_k but appear to be stabilized by intermolecular N−H$\cdots$O=C or N−H$\cdots$S=C hydrogen bonds. In the crystal, the C=O or C=S bonds makes a dihedral angle with the adjacent phenyl ring: 2DBA, 19.4°; 3DBA, 27.6° and 33.5°; 2DBTA, 39.3° and 38.7°; 3DBTA, 43.0° and 33.3°.

Our studies[31] have shown that polymeric chains without aromatic groups and strong intermolecular interactions as well as their model compounds tend to crystallize in the most stable conformation predicted from MO calculations for the models. This is not the case with the aromatic polyamides and polythioamides because of the strong intermolecular N−H$\cdots$O=C

Table 7 Solubilities of PA2T, PA3T, PTA2T, and PTA3T[a]

solvent[b]	PA2T	PA3T	PTA2T	PTA3T
water	–	–	–	–
methanol	–	–	–	–
ethanol	–	–	–	–
chloroform	–	–	–	–
dichloromethane	–	–	–	–
tetrahydrofuran	–	–	–	–
$NaOH_{aq}$	–	–	–	–
triethylamine	–	–	–	–
piperidine	–	–	–	–
pyridine	–	–	+	+
DMF	–	–	+	+
DMAc	–	–	+	+
DMSO	–	–	+	+
NMP	–	–	+	+
HFIP	+	+	+	+
phenol	–	±	±	±
TFA	+	+	+	+
sulfuric acid	+	+	+	+

[a]Symbols: +, soluble at ambient temperature; ±, soluble at elevated temperatures; —, insoluble. [b]Abbreviation: $NaOH_{aq}$, sodium hydroxide aqueous solution; DMF, *N,N*-dimethylformamide; DMAc, *N,N*-dimethylacetamide; DMSO, dimethyl sulfoxide; NMP, *N*-methylpyrrolidone; HFIP, 1,1,1,3,3,3-hexafluoro-2-propanol; TFA, trifluoroacetic acid.

or N–H···S=C attractions.

3.9 X-ray diffraction

Fig. 10 shows powder X-ray diffraction patters observed from annealed samples of the polyamides and polythioamides. The annealing was conducted for 2 h under reduced pressure at 150° much higher than T_g (see below). The polyamides exhibited broad peaks around $2\theta = 15 - 30°$ and 43°, which indicate the existence of distorted crystallites. On the other hand, the polythioamides yielded a broad amorphous halo around 20°.

3.10 Thermal analysis

Fig. 11 shows TG curves of PA2T, PTA2T, PA3T, and PTA3T. The thermal decomposition temperatures (T_d's) were determined as follows: PA2T, 421 °C; PA3T, 391 °C; PTA2T, 261 °C; PTA3T, 250 °C. The polyamides are superior to the polythioamides in thermal resistance. The glass transition temperatures detected by DSC are 52 °C (PA2T), 30 °C (PA3T), 23 °C (PTA2T), and 10 °C (PTA3T). Shashoua and Eareckson[12] determined melting points of PA2T and PA3T to be 455 and 399 °C, respectively; however, these temperatures probably correspond to our T_d's.

The equilibrium melting point T_m^0 is related to the enthalpy (ΔH_u) and entropy (ΔS_u) of fusion by

$$T_m^0 = \frac{\Delta H_u}{\Delta S_u} \quad (5)$$

The S_{conf} values of the polyamides and polythioamides treated here are comparatively large (see Table 6), and hence ΔS_u would also be large because S_{conf} accounts mostly for ΔS_u (*e.g.,* 80–90% in polyethers[31] and 65–75% in polyesters[3]). From Table 6, it is seen that the S_{conf} value of $P2TS_2$ in particular is small. This is because the $P2TS_2$ chain exclusively adopts the g^+tg^- conformation to be rigid and extended; therefore, its $< r^2 >_0 / nl^2$ value is as large as 16.7. Consequently, $P2TS_2$ does not melt up to the thermal decomposition at 346 °C although it is semicrystalline. The two polyamides of low crystallinity, PA2T and PA3T, also exhibit no melting. The reason for no fusion possibly stems from another factor, ΔH_u. The ΔH_u value, due to the strong intermolecular N-H···O=C hydrogen bonds and π/π and C-H···π attractions, may be so large a negative that the T_m's would be higher than T_d's.

The aromatic polydithioesters except $P3TS_4$ and $P4TS_4$ are amorphous,[5] and so are the polythioamides treated here. This is partly due to the flexible rotation around the benzene ring. The six orientations with small energy differences (at most, 0.5 kcal mol^{-1}) prevent the polymers from crystallizing into a single state. In addition, the large van der Waals radius of sulfur disturbs effective intermolecular π/π stackings. Because electronegativities of carbon sulfur, and oxygen are, re-

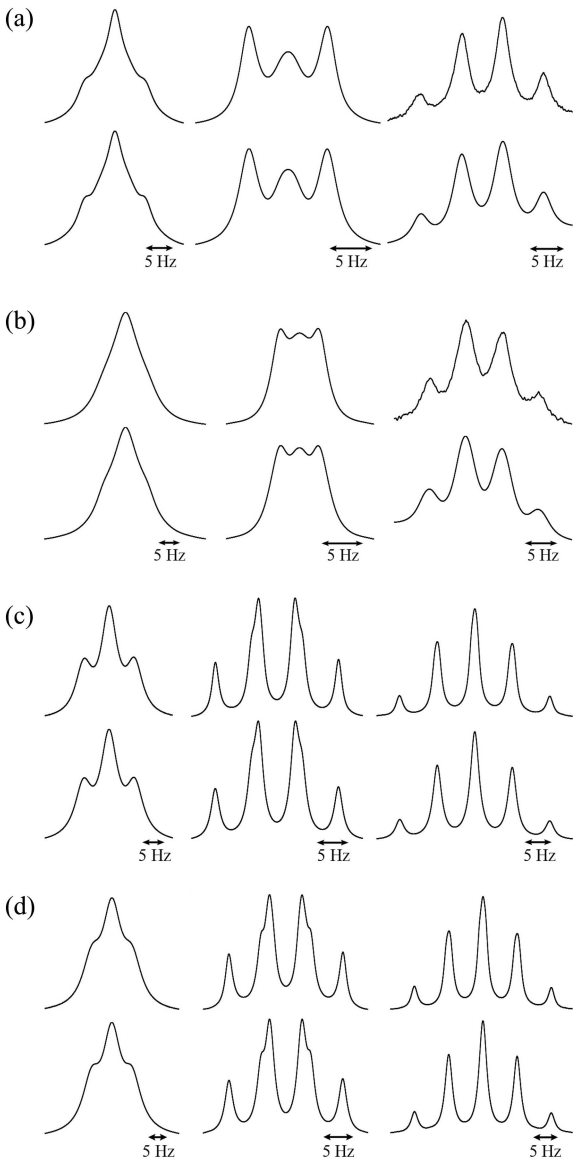

Fig. 4 Observed (above) and calculated (below) ^{1}H NMR spectra of (a) 2DBA, (b) 2DBTA, (c) 3DBA, and (d) 3DBTA: left, NH proton; center, H_A and $H_{A'}$; right, H_B and $H_{B'}$.

spectively, 2.5, 2.5, and 3.5, the dipole moment of the amide group exceeds that of the thioamide part and, consequently, the dipole-dipole interactions of the C=S polymers are also weaker than those of the C=O ones.

4 Concluding remarks

Conformational characteristics of the aromatic polyamides and polythioamides have been predicted from NMR experiments and MO calculations on the model compounds. The

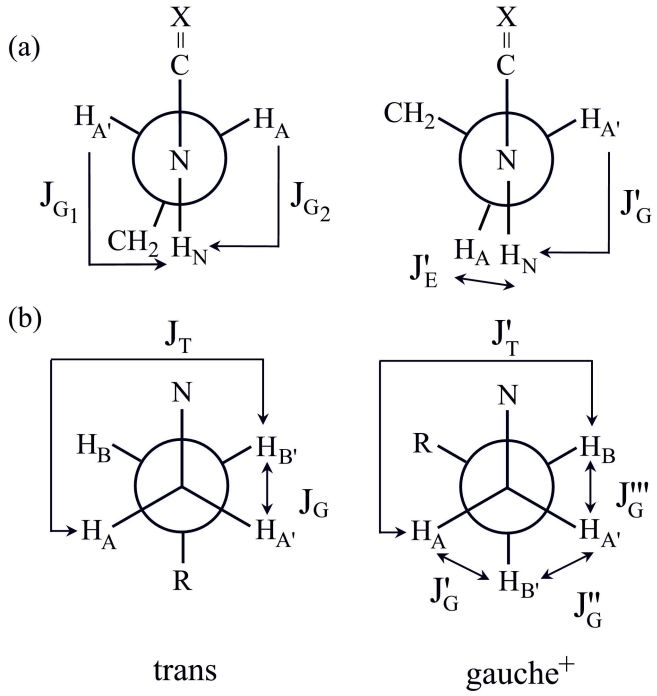

Fig. 5 Rotational isomeric states around the (a) N–CH_2 and (b) CH_2–CH_2 bonds of the model compounds with definition of vicinal trans (J_T) and gauche (J_G) coupling constants.

comparison between the NMR and MO data showed that the B3LYP functional yielded more reliable results than the MP2 theory. The MP2 calculations may overestimate the π/π and C-H$\cdots\pi$ attractions and unsatisfactorily reproduce effects of the helix-breaking and polar solvents. The B3LYP energies and geometrical parameters were applied to the refined RIS scheme to evaluate configurational properties and thermodynamic quantities of the polyamides and polythioamides.

The polyamides were synthesized by interfacial polycondensation, and the polythioamides by the Willgerodt-Kindlet type reaction. The polymers were characterized in terms of solubility, molecular weight, crystallinity, thermal stability, and thermal transition. The experimental results were compared with those of the aromatic polyesters, polythioesters, and polydithioesters.

In general, the C=O polymers (polyesters, polythioesters, and polyamides) are superior in thermal stability but inferior in solubility to the C=S ones (polydithioesters and polythioamides). This is probably due to the difference in thermal resistance between the functional groups and partly due to those between the former and latter polymers in intermolecular hydrogen bond and configurational entropy (S_{conf}). The magnitude of S_{conf} depends on not only intramolecular interactions such as the hydrogen bonds, π/π and CH$\cdots\pi$ attractions, and dipole–dipole interactions but also the ro-

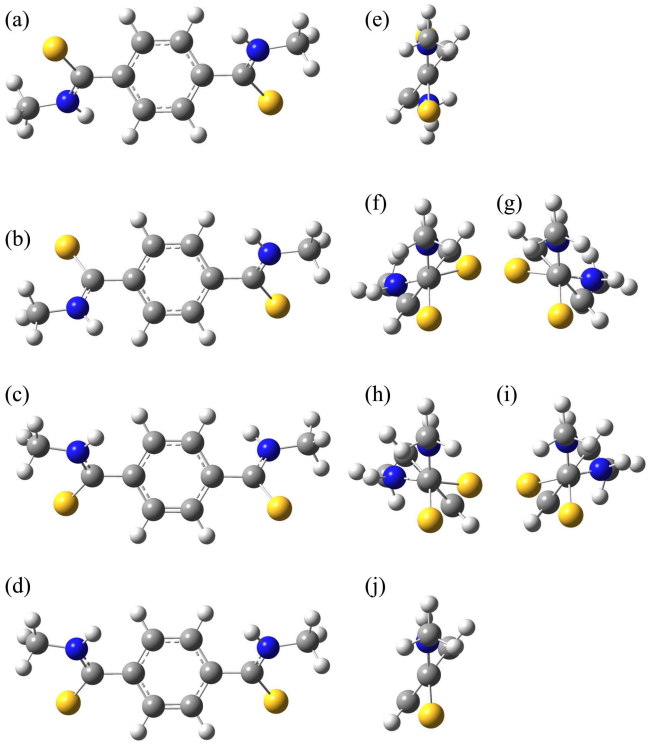

Fig. 6 Rotational isomeric states around bonds 3 and b: top views, (a) trans-trans (abbreviated as t-t), (b) trans-cis (t-c), (c) cis-trans (c-t), and (d) cis-cis (c-c); side views, (e) t-t, (f) $(t\text{-}c)^{+}$, (g) $(t\text{-}c)^{-}$, (h) $(c\text{-}t)^{+}$, (i) $(c\text{-}t)^{-}$, and (j) c-c. The model compound shown here is *N,N'*-dimethylterephthalamide (X = O) or *N,N'*-dimethylterephthalthioamide (X = S). The first (left) symbol of the six states represents the relative orientation between the C=O (C=S) bonds, and the second (right) expresses whether the two C=O (C=S) bonds project on the same (cis) side or opposite (trans) sides with respect to the benzene plane. The signs, + and −, stand for the rotational directions of the dihedral angle, being similar to those of g^{+} and g^{-}.

tation of the C=O or C=S bond around the benzene ring. The polyesters and polythioesters have only two orientations (trans and cis) between the C=O groups bonded to the same benzene ring, while the polydithioesters, polyamides, and polythioamides exhibit six orientations of trans-trans, $(trans\text{-}cis)^{\pm}$, $(cis\text{-}trans)^{\pm}$, and cis-cis. Hence, the C=O polymers are semicrystalline, and the C=S ones are amorphous or of very low crystallinity and optically translucent.

In a series of studies, we have investigated the aromatic polymers expressed as $[\text{-}C(=X)C_6H_4C(=X)\text{-}Y\text{-}(CH_2)_y\text{-}Y\text{-}]_x$ (X = O or S and Y = O, S, or NH) and found that these polymers, depending on the combination of X and Y, show different conformational characteristics, which lead to various higher-order structures and physical properties.

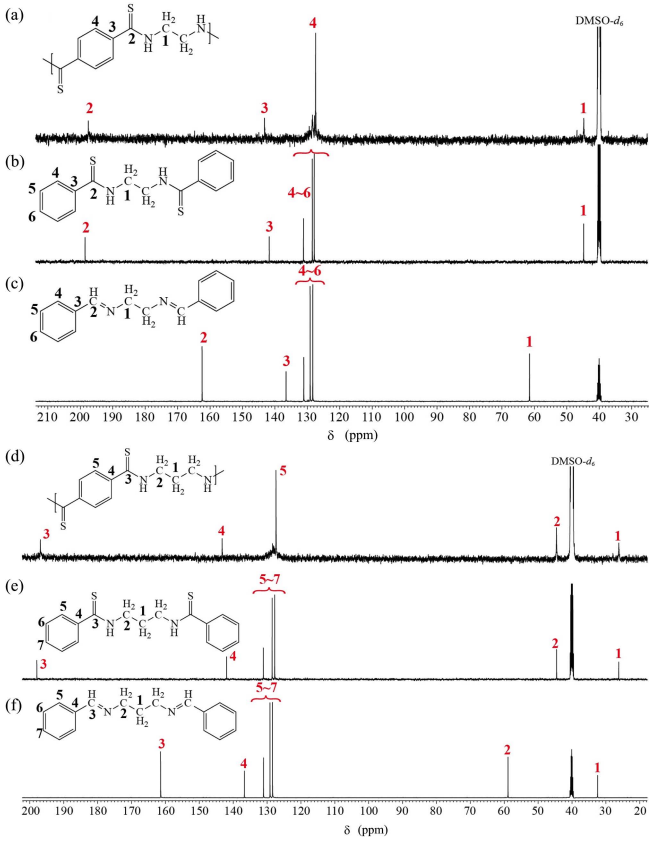

Fig. 7 Solution ^{13}C NMR spectra observed from (a) PTA2T and (d) PTA3T dissolved in DMSO-d_6, compared with those from (b) 2DBTA, (c) DB2A, (e) 3DBTA, and (f) DB3A. The peaks were assigned as indicated.

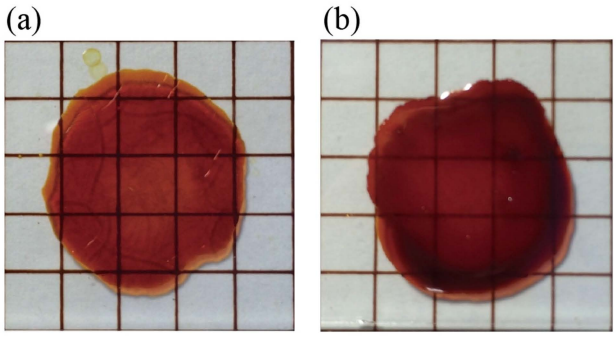

Fig. 8 Films cast from DMF solutions: (a) PTA2T and (b) PTA3T.

Acknowledgements

We thank Mr. Ezawa and Mr. Kodaira of Japan Analytical Industry Co., Ltd. for the SEC measurements. This study was partly supported by a Grant-in-Aid for Scientific Research (C) (22550190) from the Japan Society for the Promotion of Science.

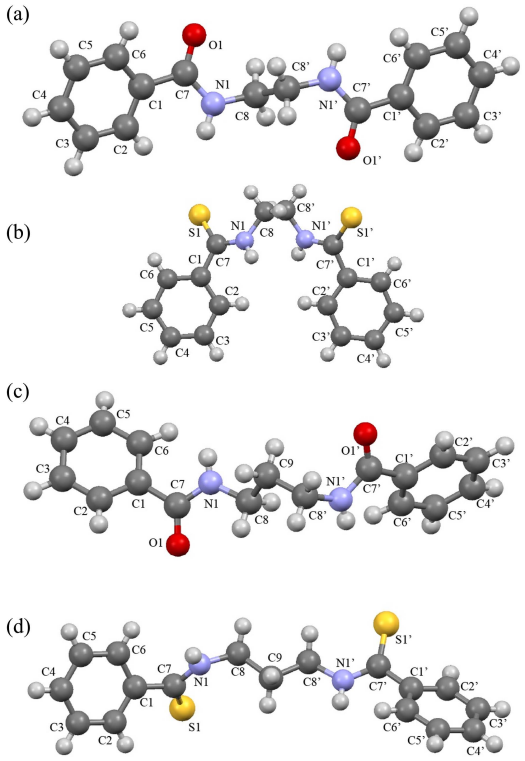

Fig. 9 Crystal conformations of (a) 2DBA (in g^+tg^-), (b) 2DBTA ($g^+g^+g^+$), (3) 3DBA (ttg^+g^+), and (d) 3DBTA ($tttg^+$).

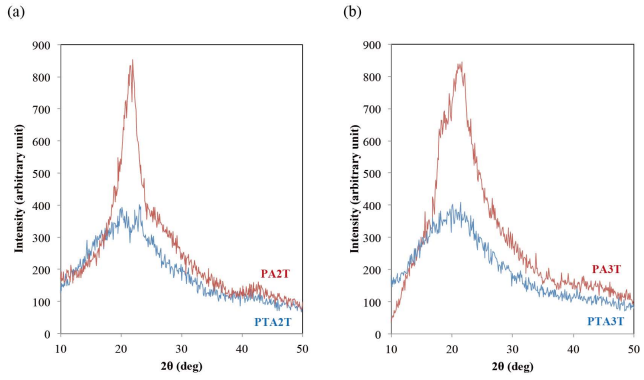

Fig. 10 Powder X-ray diffraction diagrams: (a) PA2T and PTA2T; (b) PA3T and PTA3T.

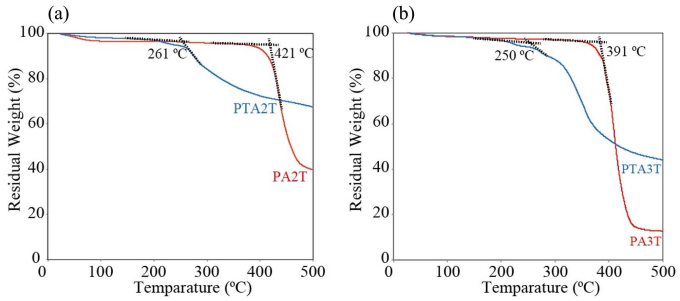

Fig. 11 Thermogravimetric (TG) diagrams: (a) PA2T and PTA2T; (b) PA3T and PTA3T. The pyrolysis temperature was determined from the intersection of two tangents on the TG curve before and after the beginning of the weight loss as shown.

References

1 Y. Sasanuma, *Macromolecules*, 2009, **42**, 2854–2862.
2 Y. Sasanuma and N. Suzuki, *Macromolecules*, 2009, **42**, 7203–7212.
3 Y. Sasanuma, Y. Wagai, N. Suzuki and D. Abe, *Polymer*, 2013, **54**, 3904–3913.
4 D. Abe and Y. Sasanuma, *Polym. Chem.*, 2012, **3**, 1576–1587.
5 D. Abe, Y. Fukuda and Y. Sasanuma, *Polym. Chem.*, 2015, **6**, 3131–3142.
6 P. J. Flory, *Statistical Mechanics of Chain Molecules*, Wiley & Sons, New York, 1969.
7 W. L. Mattice and U. W. Suter, *Conformational Theory of Large Molecules: The Rotational Isomeric State Model in Macromolecular Systems*, Wiley-Interscience, New York, 1994.
8 Y. Sasanuma, S. Asai and R. Kumagai, *Macromolecules*, 2007, **40**, 3488–3497.
9 A. R. Jacobson, A. N. Makris and L. M. Sayre, *J. Org. Chem.*, 1987, **52**, 2592–2594.
10 H. Hart and J. L. Brewbaker, *J. Am. Chem. Soc.*, 1969, **91**, 706–711.
11 M. P. Cava and M. I. Levinson, *Tetrahedron*, 1985, **41**, 5061–5087.
12 V. E. Shashoua and W. M. Eareckson, *J. Polym. Sci.*, 1959, **40**, 343–358.
13 T. Kanbara, Y. Kawai, K. Hasegawa, H. Morita and T. Yamamoto, *J. Polym. Sci.: Part A: Polym. Chem.*, 2001, **39**, 3739–3750.
14 A. Simion, C. Simion, T. Kanda, S. Nagashima, Y. Mitoma, T. Yamada, K. Mimura and M. Tashiro, *J. Chem. Soc., Perkin Trans. 1*, 2001, 2071–2078.
15 P. H. Budzelaar, *gNMR*, version 5.0, IvorySoft & Adept Scientific plc, Letchworth, U.K., 2004.
16 M. J. Frisch, G. W. Trucks, H. B. Schlegel, G. E. Scuseria, M. A. Robb, J. R. Cheeseman, G. Scalmani, V. Barone, B. Mennucci, G. A. Petersson, H. Nakatsuji, M. Caricato, X. Li, H. P. Hratchian, A. F. Izmaylov, J. Bloino, G. Zheng, J. L. Sonnenberg, M. Hada, M. Ehara, K. Toyota, R. Fukuda, J. Hasegawa, M. Ishida, T. Nakajima, Y. Honda, O. Kitao, H. Nakai, T. Vreven, J. A. Montgomery, Jr., J. E. Peralta, F. Ogliaro, M. Bearpark, J. J. Heyd, E. Brothers, K. N. Kudin, V. N. Staroverov, R. Kobayashi, J. Normand, K. Raghavachari, A. Rendell, J. C. Burant, S. S. Iyengar, J. Tomasi, M. Cossi, N. Rega, J. M. Millam, M. Klene, J. E. Knox, J. B. Cross, V. Bakken, C. Adamo, J. Jaramillo, R. Gomperts, R. E. Stratmann, O. Yazyev, A. J. Austin, R. Cammi, C. Pomelli, J. W. Ochterski, R. L. Martin, K. Morokuma, V. G. Zakrzewski, G. A. Voth, P. Salvador, J. J. Dannenberg, S. Dapprich, A. D. Daniels, O. Farkas, J. B. Foresman, J. V. Ortiz, J. Cioslowski and D. J. Fox, *Gaussian 09 Revision B.01*, Gaussian Inc. Wallingford CT 2009.
17 A. D. Becke, *J. Chem. Phys.*, 1993, **98**, 5648–5652.
18 M. Cossi, N. Rega, G. Scalmani and V. Barone, *J. Comp. Chem.*, 2003, **24**, 669–681.
19 C. Møller and M. S. Plesset, *Phys. Rev.*, 1934, **46**, 618–622.
20 Y. Zhao and D. G. Truhlar, *Theor. Chem. Acc*, 2008, **120**, 215–2412.
21 T. Helgaker, M. Watson and N. C. Handy, *J. Chem. Phys.*, 2000, **113**, 9402–9409.
22 *IUPAC. Compendium of Chemical Terminology, 2nd ed. (the "Gold Book")*, ed. A. D. McNaught and A. Wilkinson, Blackwell Scientific Publications, Oxford, UK, 1997.

23 A. Pardi, M. Billeter and K. Wüthrich, *J. Mol. Biol.*, 1984, **180**, 741–751.
24 S. Ludvigsen, K. V. Andersen and F. M. Poulsen, *J. Mol. Biol.*, 1991, **217**, 731–736.
25 Y. Sasanuma, S. Hattori, S. Imazu, S. Ikeda, T. Kaizuka, T. Iijima, M. Sawanobori, M. A. Azam, R. V. Law and J. H. G. Steinke, *Macromolecules*, 2004, **37**, 9169–9183.
26 Y. Sasanuma, F. Teramae, H. Yamashita, I. Hamano and S. Hattori, *Macromolecules*, 2005, **38**, 3519–3532.
27 S. Tsuzuki, K. Honda, T. Uchimaru, M. Mikami and K. Tanabe, *J. Am. Chem. Soc.*, 2002, **124**, 104–112.
28 E. C. Lee, D. Kim, P. Jurečka, P. Tarakeshwar, P. Hobza and K. S. Kim, *J. Phys. Chem. A*, 2007, **111**, 3446–3457.
29 C. A. Morgado, P. Jurečka, D. Svozil, P. Hobza and J. Šponer, *Phys. Chem. Chem. Phys.*, 2010, **12**, 3522–3534.
30 M. Pitoňák, P. Neogrády, J. Černý, S. Grimme and P. Hobza, *ChemPhysChem*, 2009, **10**, 282–289.
31 Y. Sasanuma, A. Watanabe and K. Tamura, *J. Phys. Chem. B*, 2008, **112**, 9613–9624.
32 S. Grimme, *WIREs Comput. Mol. Sci.*, 2011, **1**, 211–228.
33 A. Palmer and F. Brisse, *Acta Crystallogr.*, 1980, **B36**, 1447–1452.
34 J. Brisson and F. Brisse, *Macromolecules*, 1986, **19**, 2632–2639.
35 M. Nagasawa, Y. Sasanuma and H. Masu, *Acta Crystallogr.*, 2014, **E70**, o586.
36 M. Nagasawa, Y. Sasanuma and H. Masu, *Acta Crystallogr.*, 2014, **E70**, o639.

Graphical abstract Structure and properties of aromatic polyamides and polythioamides were investigated and compared with those of analogous polyesters, polythioesters, and polydithioesters.

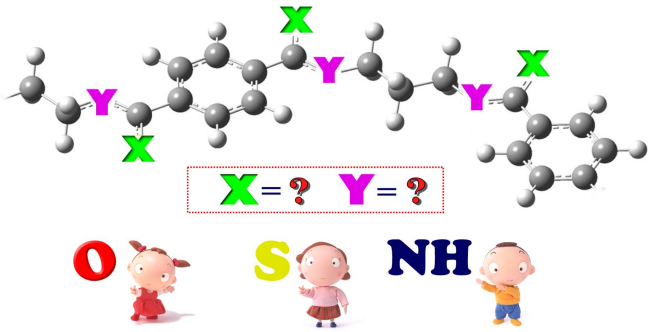

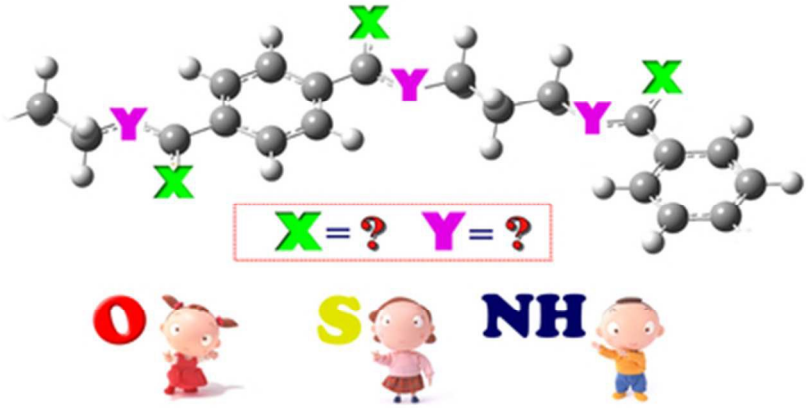

37x17mm (300 x 300 DPI)